*J. Fluid Mech.* (2006), *vol.* 550, *pp.* 185–205. © 2006 Cambridge University Press
doi:10.1017/S0022112005008219 Printed in the United Kingdom


# Active control of boundary-layer instabilities

By YONG LI AND MICHAEL GASTER

Department of Engineering, Queen Mary, University of London, Mile End Road, London E1 4NS, UK

(Received 15 February 2005 and in revised form 19 August 2005)

Active control of spatially evolving three-dimensional instability waves in the boundary layer of a flat plate with zero pressure gradient has been investigated both numerically and experimentally. The boundary layer was artificially excited by various computer-generated perturbations in a low-turbulence wind tunnel so as to create a three-dimensional field of instability waves. Sensors were used to detect the oncoming disturbances and appropriate control signals sent to the downstream actuators to generate counteracting disturbances. The key element of this type of active control is the determination of the transfer function of the control system connecting the sensors with the actuators. Modelling by linear theory showed that the amplitudes of the disturbances downstream were significantly suppressed when the causal transfer function was applied. To simplify the control problem different strategies using approximations to the transfer function were used. It was shown that with a very simple transfer function almost the same result could be achieved as with the full causal transfer function. The modelling was validated experimentally, first by an *off-line* control using different control modes, i.e. different transfer functions, and then by a *real-time* hardware implementation using one of the modes. Good agreement between the experimental measurements and numerical predictions indicated that a simple control strategy could be developed to inhibit the growth of the three-dimensional instability waves over extensive regions of the flow.

## 1. Introduction

Transition on aircraft wings from a laminar boundary layer to a turbulent one generally occurs through the amplification of naturally excited instability waves. In flows where the external turbulence is high and large perturbations are created in the boundary layer the near-field transient component may initiate transition without any modal growth of the eigensolutions. Here we consider only low excitation levels that can be expected to arise on aircraft wings, and then the most likely mechanism for eventual transition to turbulence is through the amplification of travelling eigenmodes. The resulting turbulent boundary layer has considerably larger skin friction than that of the laminar flow, inevitably increasing the drag of the aircraft and therefore the fuel consumption. The ability to reduce the skin friction can provide economic and environmental advantages. Delaying transition and maintaining a laminar flow as long as possible on the wings results in lower drag, better fuel efficiency and, more importantly, less upper atmospheric pollution.

A worldwide interest in the problem of transition control developed in the 1930s–1990s. Some techniques used to control the laminar–turbulent transition process in the boundary layer are passive, requiring modification to the mean flow in order to inhibit the growth of disturbance waves. These approaches include pressure-gradient

modification, mean surface-temperature control and localized steady surface suction, etc. (Saric 1992; Braslow 1999). Since in a low noise environment laminar–turbulent transition arises from the growth of instability waves, active control can also be used to suppress the natural disturbances by dynamically interfering with the instability waves. The most common approach has been to use active wave cancellation, where the wave-like disturbances can be linearly cancelled by the introduction of another wave of equal amplitude but opposite phase. One advantage of this technique is that effective control can be achieved with only a small expenditure of energy.

The early work by Milling (1981), using two vibrating wires, and by Liepmann, Brown & Nosenchuck (1982*a*, *b*), using two heating strips in a water channel, showed that some degree of control could indeed be achieved. One wire or strip worked as an excitation source and the other one as an actuator. Later, Thomas (1983) repeated the earlier water-tunnel experiments in a wind tunnel. All the experiments showed that by appropriate adjustment of the phase and amplitude of the signal driving the second actuator, an-order-of-magnitude reduction in the two-dimensional primary disturbance amplitude could be obtained and some transition delay realized. However, the downstream wave was never exactly annihilated and some residue remained. The flow could not therefore be restored completely to its undisturbed state. Recent experimental work of Sturzebecher & Nitsche (2003) showed that a sensor–actuator system combined with an adaptive control algorithm could successfully be used to achieve a powerful attenuation of naturally excited two-dimensional Tollmien–Schlichting (T-S) instabilities on an unswept wing. With a pure two-dimensional control system a local T-S wave was reduced in amplitude by about 90 %. They also claimed that three-dimensional instabilities were successfully cancelled by means of a spanwise arrangement of sensors and actuators. In order to study the effect of nonlinearity and three-dimensionality of the travelling disturbances on the performance of active wave cancellation, Opfer *et al.* (2003) developed two different active-control systems in a zero-pressure-gradient laminar boundary layer. By adding nonlinearity or special three-dimensional modelling capabilities to the system some minor improvement in performance was achieved, but at high computational cost.

In addition to the experimental work, there have been various evaluations of the active-control concept using numerical experimentation aimed at understanding the physics of the wave-cancellation process. Based on the Navier–Stokes (N-S) equations, Biringen (1984) used a temporally growing instability formulation in a parabolic channel flow. By using periodic suction and blowing on the boundary as the control the amplitudes of two-dimensional disturbance waves were found to be reduced by approximately 50 %. Some reduction of the three-dimensional instabilities was also obtained. Kral & Fasel (1991) used solutions of the N-S equations with spatial modes to study the effect of unsteady heating on unstable two-dimensional and three-dimensional waves travelling in a non-parallel laminar-boundary-layer flow on a flat plate. Their study showed that transition could be delayed by superposing anti-phase disturbances or be accelerated by introducing in-phase disturbances. They also showed that control was most effective when applied at an early stage of wave growth, i.e. in the linear regime. Within the limits of linear stability theory and the parallel-flow assumption, Bower *et al.* (1987) and Pal, Bower & Meryer (1991) considered the two-dimensinal Orr–Sommerfeld (O-S) equation in designing an input to channel flow that could be used to counteract the effects of a disturbance that supported instabilities. They showed that if an oscillation at the lower boundary of a channel excited inherent instability waves (even multi-frequency waves), a second oscillation could be constructed downstream to generate the cancelling waves that

negated the instabilities. Laurien & Kleiser (1989) and Kleiser & Laurien (1985) reported two- and three-dimensional studies for boundary-layer flows and Poiseuille flow, respectively. If the anti-phase control was introduced at an early stage of the process, they were able to reduce two-dimensional fluctuation amplitudes by nearly an order of magnitude and thus delay the onset of the transition. They, however, also noted that the two-dimensional control was no longer successful in the later strongly three-dimensional stage, where three-dimensional wave interactions were dominant.

Joslin *et al.* (1995) and Joslin, Erlebacher & Hussaini (1996) used DNS (direct numerical simulation) to show that wave cancellation was the fundamental reason for the reduction in amplitudes of the instability waves. They explained that the wave cancellation was very sensitive to the wave parameters and postulated that incomplete reduction in the controlled motion, reported in the earlier studies, arose from imperfect phase or amplitude properties of the cancelling wave. Gmelin & Rist (2001) examined different active approaches in various flow scenarios using both DNS and linear stability theory. They showed that the superposition of disturbances with opposite phase on the initial waves in the boundary layer led to a significant attenuation only in linear and weakly nonlinear scenarios. In stages close to transition, where strong nonlinearity has already taken place, the instantaneous feedback vorticity control led to better damping of nonlinear disturbances. Instead of using DNS, Gaster (2000) used linear stability theory to investigate the possibility of active control of spatially evolving instability waves in the boundary layer of a flat plate. In order to lead to a practical implementation, both two- and three-dimensional control strategies were developed. It was shown that a useful amount of control could be obtained using practical spacing of the sensors and controlling actuators distributed on the plate surface.

A global approach to the control problem has been tackled by a number of authors. Bewley & Liu (1998) showed that the instabilities in channel flow could be suppressed by applying suitable active boundary value control in response to some measurable function on the surface. This theoretical approach was then validated by numerical modelling. These idea have been also applied to spatially evolving boundary layers (Högberg & Henningson (2002) and also by Walther, Airiau & Bottaro (2001). Linear optimal control theory was used to determine an estimator-based feedback to maintain laminar flow. Numerical modelling has shown the power of this approach in significantly reducing the level of the disturbances. The feasibility of applying these control strategies to real flows has been discussed by Bewley (2001), but practical implementation seems only likely in the future as vast numbers of sensors and actuators appear to be necessary.

Most investigations have focused on two-dimensional periodic disturbances. Theoretical methods have generally been used because of the difficulties in carrying out suitable experiments. Here we investigate the control of three-dimensional artificially excited disturbances following the work reported briefly by Gaster (2000). A similar approach to the earlier work has been used to determine the test geometry and the control strategy for cancelling the three-dimensional disturbance field. Our aim has been to shown that a very simple, thus practical and cheap, control approach can produce worthwhile results. Implementation on a large domain is thus a possibility. Disturbances were artificially introduced into the boundary layer so as to create simulated natural excitations. An array of buried speakers was positioned across the span to mimic the receptivity process of the naturally excited disturbances that were to be cancelled. By creating the upstream disturbances artificially there was not only complete control of the imposed wave field, but the experiment could

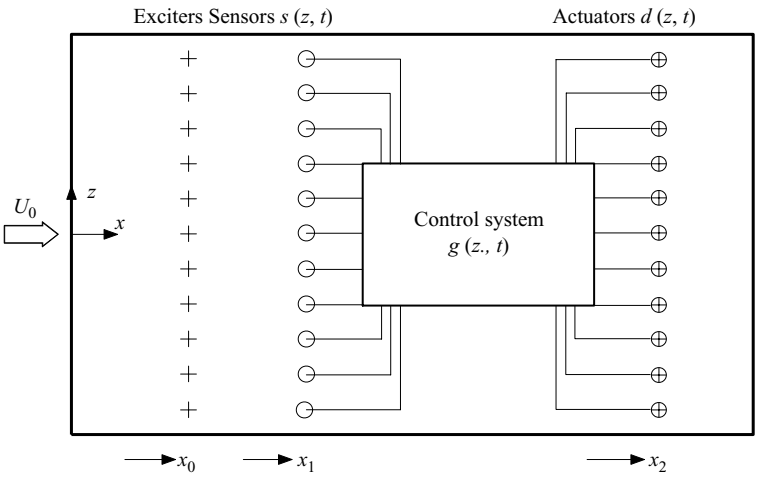


FIGURE 1. The schematic set-up of the multi-input-multi-output (MIMO) control system on the surface of a flat plate. $x_0$, $x_1$, $x_2$ represent the streamwise distances of the exciters, the sensors and the actuators from the leading edge respectively.

then be carried out deterministically. The downstream evolution of the artificial disturbances was modelled by the linearized perturbation equations using the parallel-flow approximation. Suitable disturbances were then introduced into the flow at some downstream locations to cancel this unstable flow field. By carrying out numerical simulation and experiments under the same flow conditions, it was possible to highlight the mechanisms of the control process and therefore assess the practicability of any control scheme.

## 2. Control modelling and strategies

The control scheme to be modelled is shown in figure 1. In order to account for the three-dimensional characteristics of the disturbances, a multi-input-multi-output (MIMO) control system was constructed to cancel the on-coming instability waves. The streamwise position, $x$, is defined as distance from the leading edge of the plate and the spanwise position, $z$, from the centreline. Disturbances were introduced by the upstream array of jet-type exciters. The sensor signal, $s(z, t)$, at each spanwise position was convolved in both space and time with the transfer function, $g(z, t)$, of the control system to provide the control signal, $d(z, t)$, driving the downstream actuator (also a jet-type source) array. The cancelling signals, $c(z, t)$, at the positions downstream of the actuator array were obtained by convolving the driving signal with the full impulse response of the boundary layer.

### 2.1. *Numerical method*

The simulation of the developing disturbances in the boundary layer was calculated in a rectangular integration domain with the spatial codes developed by Gaster & Shaikh (1996). The flow field created by a localized velocity boundary value on the wall, such as a periodic jet, can be modelled reasonably well by the linearized perturbation equations on a parallel mean base flow. This approximation enables the equations to be separated so that Fourier transforms in time, and streamwise and spanwise

space can be taken. The problem was cast in a velocity–vorticity form to create a set of six equations for the six unknowns. These equations can readily be integrated and the appropriate boundary value incorporated. The resulting solutions in terms of velocities and vorticities arise as separate components from the continuous spectrum and the eigensolutions from the singular element in the integral transform inversion. This is convenient because our interest is in controlling the unstable eigenmodes and no attempt is made to control either the near-field or the decaying travelling waves. Comparisons of the streawise velocity perturbations generated by a periodic jet have been made with predictions from the model. Close to the source agreement was found to be excellent, but far downstream, where the boundary layer has grown, agreement was somewhat qualitative. The theoretical model can only provide useful predictions for weak excitations. A paper describing this work is in preparation.

The streamwise and spanwise directions were discretized at 1 mm intervals and in the wall-normal direction, $y$, a non-dimensional $\eta = y(U_0/\nu x)^{1/2}$ was used. The perturbation equations were integrated by a standard Runge–Kutta fourth-order scheme from the outer-boundary condition marching towards the wall boundary. The variables were normalized with respect to the mean velocity, $U_0 = 12\,\mathrm{m\,s^{-1}}$, the kinematic viscosity $\nu = 1.4573 \times 10^{-5}\,\mathrm{m\,s^{-2}}$ and the boundary-layer displacement thickness $\delta^*$ at the location of the excitation source. The exciters were positioned at $x_0 = 410\,\mathrm{mm}$ downstream from the leading edge of the flat plate and thus the Reynolds number $Re$ based on $\delta^*$ was set to 1000.

### 2.2. *Transfer function*

It was necessary to determine the link between an on-coming disturbance wave system, sensed at $x_1$, and the required action of the actuators at $x_2$ to generate the cancelling motion far downstream. In the modelling phase of the project it was assumed that the electro-mechanical transfer functions linking the surface vorticity at the sensor position to the output voltage from the sensor as well as the relationship between the applied control voltage and the jet mass flow were both unity.

In the experiment both of these transfer functions were reasonably flat over the frequency range of interest and the only influence on the control was the value of the gain. The gain required to obtain the best cancelling performance at a downstream station was found by experiment.

It is first convenient to consider two-dimensional disturbances in order to find the transfer function of the control system. A disturbance with a surface vorticity$(x, t)$ can be defined in Fourier space

$$\text{vorticity}(x, t) = \int V(\omega)\, \mathrm{e}^{\mathrm{i}\alpha(\omega)x} \mathrm{e}^{-\mathrm{i}\omega t}\, \mathrm{d}\omega, \tag{2.1}$$

where the spectrum, $V(\omega)\mathrm{e}^{\mathrm{i}\alpha(\omega)x}$, evolves with $x$, $\alpha(\omega)$ and $\omega$ are the streamwise wavenumber and angular frequency respectively.

In particular, the vorticity spectrum at the sensor station $(x_1)$ is

$$V(\omega)\, \mathrm{e}^{\mathrm{i}\alpha(\omega)x_1}, \tag{2.2}$$

where the eigenvalues, $\alpha(\omega)$, were calculated from the linear theory.

The controlling jet was modelled by a local wall-normal-velocity boundary value that was treated as a spatial delta function. Linear theory provided values of the resulting surface velocity spectrum generated by a unit mass impulse at $x_2$. The solution arises in two parts. There is an initial transient near the source and there is also the downstream packet of eigenmodes. Here we are only concerned with the eigenmodes

and the spectrum is given by

$$Q(\omega)\mathrm{e}^{\mathrm{i}\alpha(\omega)(x-x_2)}, \tag{2.3}$$

and for a jet of spectral content $J(\omega)$ the result downstream is

$$J(\omega)Q(\omega)\mathrm{e}^{\mathrm{i}\alpha(\omega)(x-x_2)}. \tag{2.4}$$

In order to cancel the downstream surface-vorticity fluctuation it is necessary to choose $J(\omega)$ so that

$$J(\omega)Q(\omega)\mathrm{e}^{\mathrm{i}\alpha(\omega)(x-x_2)} \equiv -V(\omega)\mathrm{e}^{\mathrm{i}\alpha(\omega)x}. \tag{2.5}$$

Therefore, the transfer function, $G(\omega)$, relating the jet mass flow spectrum, $J(\omega)$, to the sensor spectrum is

$$G(\omega) = \frac{J(\omega)}{V(\omega)\mathrm{e}^{\mathrm{i}\alpha(\omega)x_1}} = \frac{-\mathrm{e}^{\mathrm{i}\alpha(\omega)(x_2-x_1)}}{Q(\omega)}. \tag{2.6}$$

In the three-dimensional case we get

$$G(\beta, \omega) = \frac{-\mathrm{e}^{\mathrm{i}\alpha(\beta,\omega)(x_2-x_1)}}{Q(\beta, \omega)}, \tag{2.7}$$

and in the physical phase

$$g(z, t) = \iint G(\beta, \omega)\mathrm{e}^{\mathrm{i}\beta z}\mathrm{e}^{-\mathrm{i}\omega t}\,\mathrm{d}\beta\,\mathrm{d}\omega, \tag{2.8}$$

where $\beta$ represents the spanwise wavenumber.

The transfer function of the three-dimensional system, obtained solely from the unstable eigenmodes, is shown in figure 2 for two separation distances. The $\Delta x$ $(= x_2 - x_1)$ is the streamwise separation between the sensor array and the actuator array. These contour plots were evaluated for an excitation of a unit normal jet over a region of 1 mm$^2$. The portion of the transfer function that occurs at negative times cannot be used because only the sensor signal in the past is available (causality). The driving signal was therefore calculated by a convolution of the sensor signal only with that portion of the transfer function that exists at positive delay times.

### 2.3. *Performance of control*

The sensors were placed 100 mm downstream from the excitation sources, i.e. $x_1 =$ 510 mm, since it was found that shorter distances introduced a rather large and unrealistic near-field component. It was thought desirable to position the actuators as close as possible to the sensors, but this created a significant upstream nearfield from the actuator that contaminated the sensor signal. Also a much greater portion of the transfer function was lost through the causality constraint. A distance of 20 mm, i.e. $\Delta x = 20$ and $x_2 = 530$ mm, was therefore chosen to avoid the upstream feedback and to reduce the degree of non-causality. Here, only the cancellation of the surface vorticity on the plate surface was calculated, while in the experimental investigation the streamwise velocity fluctuations close to the plate surface were measured.

The control system was first tested for an excitation of a wavepacket generated by a pulsed point-source exciter on the centreline. Figure 3 shows the resulting space–time wavepackets with and without control at the streamwise station of $x = 760$ mm, i.e. 350 mm downstream of the excitation source. This form of excitation caused a wedge of disturbance waves downstream. The control achieved a significant reduction of the disturbance waves, but it is clear that the wavepacket was not completely cancelled and a weak residue of roughly the same structure remained.

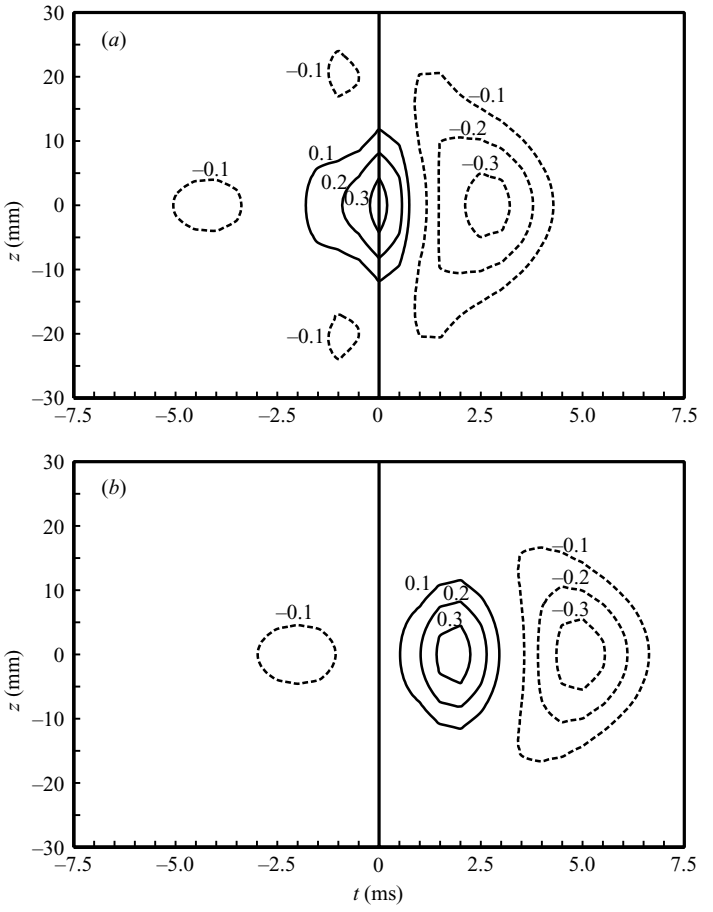


FIGURE 2. Space–time transfer functions of the three-dimensional control system at different streamwise separations ($\Delta x = x_2 - x_1$) between the upstream sensor array and the downstream actuator array. (*a*) $\Delta x = 10$ mm, (*b*) $\Delta x = 20$ mm. Dotted lines represent negative values, while solid lines refer to positive values.

The control system was then tested by exciting the boundary layer with random noise involving a broad band of frequencies from all the exciters across the span to create a three-dimensional on-coming field. The excitation source of waves was modelled by a random series of pulsed excitations distributed over a period of time and a spanwise strip of 200 mm. The original disturbances, the cancelling disturbances and the resultant after the cancellation are shown in figure 4. The original solutions and the cancelling field appear to be almost identical, thus providing excellent cancellation. The random perturbation remaining after cancellation shows that the dominant parts of the disturbances have been largely removed leaving only a small residue. The degree of success can be judged by the cross-correlation of the original with the cancelling disturbances. The average value of the correlation coefficient, $\sigma$, was found to be about 0.975, which means that the mean square of the residue after cancellation was 0.05, or $2(1-\sigma)$, of that from the original source. Therefore, roughly 75 % of the amplitude of the disturbances was cancelled with this fully three-dimensional transfer function.

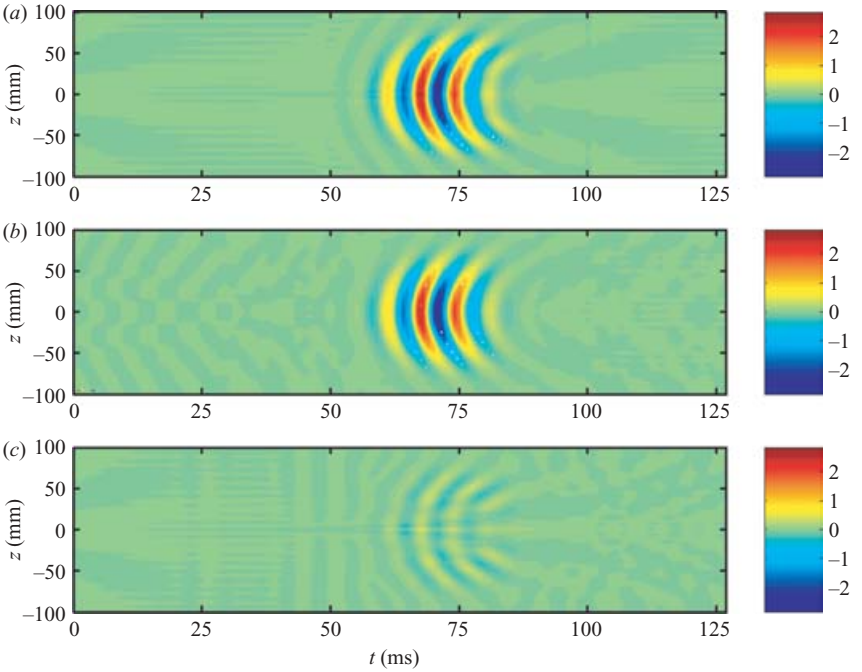


FIGURE 3. Space–time waveforms of the original surface vorticity wavepacket (*a*), the cancelling wavepacket (*b*) and the resultant (*c*) after the cancellation using the full three-dimensional transfer function. The streamwise station is 760 mm downstream from the leading edge.

### 2.4. *Control strategies*

In any practical implementation account has to be taken of the fact that the sensors and actuators are discrete devices that are strategically positioned across the span. The spanwise spacing needs to be smaller than half the minimum spanwise wavelength found in the wavenumber spectrum of the original disturbances, according to the Nyquist theorem. In other words, the spanwise distribution of the cancelling waves must be able to resolve the three-dimensional characteristics of any growing disturbances.

Various control strategies were tested by the degree of cancellation of three-dimensional random disturbances. Table 1 shows that, using the control mode of the fully three-dimensional transfer function, a correlation value of 0.974 was obtained when the spanwise spacing was less than 10 mm, with constant sampling rate of 2 kHz. At larger spacing, i.e. 20 mm, there was a rapid fall-off in correlation. The arrangement of 0.5 ms sampling period coupled with 10 mm spanwise transducer spacing is quite a practical one.

However, the full transfer function required spanwise cross-linking of all the sensors and actuators, so that each actuator would need to use the information from the neighbouring sensors as well as the one directly upstream. Cross-linking hugely increases the complexity of the control and therefore does not provide a practical scheme. Removing cross-linking means that each downstream actuator is only connected directly to an upstream sensor, and thus the transfer function between them reduces to the function on the centreline. This function can be obtained directly from two-dimensional modes ($\beta = 0$), shown in figure 5(*a*). Control with this uncoupled transfer function is defined

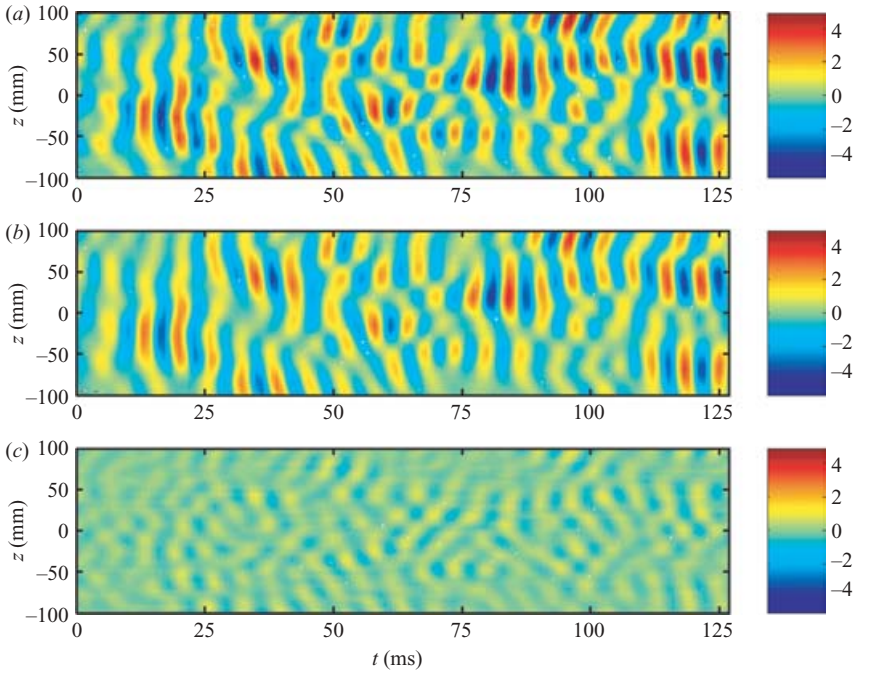


FIGURE 4. Space–time surface vorticity waveforms of the original three-dimensional random disturbances (*a*), the cancelling disturbances (*b*) and the resultant (*c*) after the cancellation using the full three-dimensional transfer function. The streamwise station is 760 mm downstream from the leading edge.

| Control mode | Span spacing (mm) | $\sigma$ |
|---|---|---|
| | 1 | 0.975 |
| | 5 | 0.975 |
| full mode† ↕ | 10 | 0.974 |
| | 15 | 0.965 |
| | 20 | 0.911 |
| mode 1‡ → | 10 | 0.972 |
| mode 2¶ → | 10 | 0.987 |
| mode 3‖ → | 10 | 0.969 |

† fully three-dimensional transfer function.
‡ uncoupled transfer function.
¶ two-spike transfer function (optimized).
‖ single-spike transfer function (optimized).

TABLE 1. Correlation coefficients ($\sigma$) at different spanwise spacing of the transducers and different control modes. $x = 760$ mm.

as mode 1 in this paper. A cross-correlation value of 0.972 (shown in table 1) was obtained after removing the cross-linking. The uncoupled transfer function was dominated by two peaks on the time axis, and thus a further simplification can be made by reducing the function to just two spikes (defined as mode 2) shown in figure 5*b*). The correlation value of 0.987 (shown in table 1) was obtained with this simple function when the magnitudes of the spikes were adjusted for optimal control. The higher value

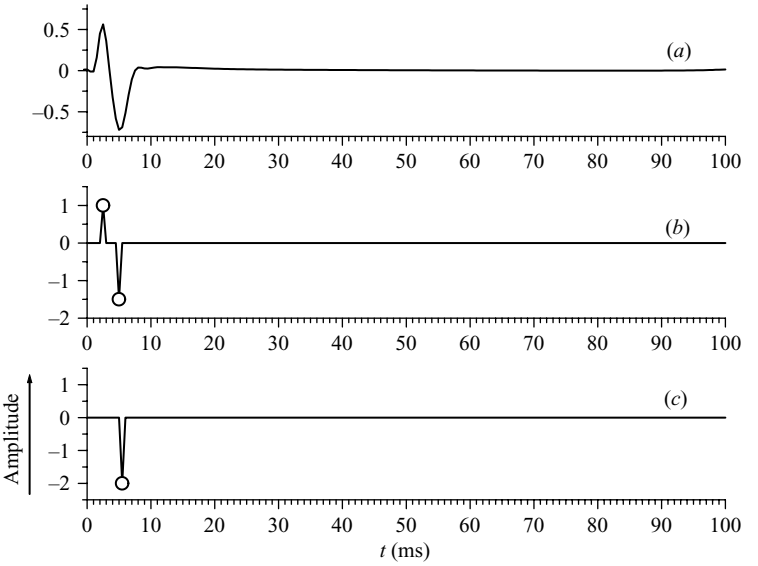


FIGURE 5. Transfer functions of the control system. (*a*) Uncoupled transfer function (mode 1); (*b*) two-spike transfer function (mode 2); (*c*) single-spike transfer function (mode 3).

of correlation was obtained because the effect of non-causality of the transfer function was offset by the optimizing process. Moreover, it was found that the second delta function played the dominant role, suggesting a further simplification to single spike. With this single-spike transfer function (defined as mode 3 shown in figure 5(*c*), whose delay time and amplitude were both optimized, the correlation value of 0.969 (shown in table 1) was obtained. The loss in effectiveness was a small price to pay for the advantages to be gained by this simplification. The convolution of this single-spike function with the sensor signal means that the driving signal is just a delayed and scaled version of the sensor signal. This is consistent with the ideas of Gmelin & Rist (2001).

### 2.5. *Model of localized control*

The control schemes discussed in the previous section require a large number of transducers distributed across the span. This was not possible to validate with only a limited number of transducers. Therefore, an experiment was set up with only a few spanwise sensors and actuators. This could only be expected to reduce the disturbances locally by a small amount. Before attempting the experiment it was important to model this local control set-up.

Predictions of the degree of control achieved with a single sensor/actuator element were rather poor even though a spanwise array of such elemental controls could be quite effective. It was found that if one sensor was coupled to three downstream actuators a rather better cancellation zone could be realized, presumably because this excitation contains weaker oblique modes. At this stage of the investigation it seemed attractive to consider an autonomous control element consisting of one sensor and three actuators. Control over a larger region could then be realized by a distribution of these elemental control devices over the surface.

Figure 6 shows the percentage cancellation of the surface vorticity with this local controller. The plus symbols represent the positions of the upstream sensor and the downstream actuators. The three downstream actuators were coupled to one

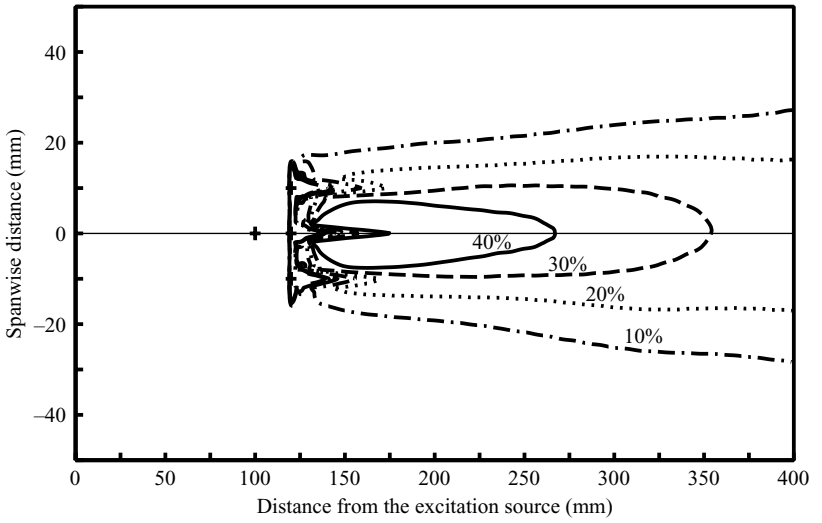


FIGURE 6. Percentage surface vorticity cancellation of the three-dimensional naturally excited disturbances in amplitudes using a local controller consisting of one sensor and three actuators. Here the streamwise distance is from the excitation source. Control mode 1 was used and the spanwise spacing of the three actuators was 10 mm. The upstream plus symbol represents the sensor and the downstream three pluses represent the three actuators.

upstream sensor, and therefore the same driving signal from the convolution of the sensor signal with the transfer function (mode 1) was used to drive the three actuators. The figure shows that a maximum cancellation of more than 40 % was obtained in the central area just downstream of the actuators. However, although the area where the disturbances could be controlled was quite narrow, it is clear that multiple spanwise devices could broaden this.

### 2.6. *Effect of external noise on control*

It was important to assess the effectiveness of the control scheme when external noise, possibly from the sensors or the electronics in the control loop, was included. A random noise signal was constructed to excite a wide spectral range of disturbances. The frequency range of the random noise was chosen to be between 80 Hz and 210 Hz, i.e. in the frequency range of unstable T-S waves. This signal was added, in various proportions, to the control signals with different signal-to-noise ratios (SNR). The performance of the local controller is shown in figure 7 using a control signal with an SNR value of 10:1. The cancellation was only slightly degraded compared with that in figure 6. An SNR of 10:1 can easily be achieved with the conventional hot-wire probe or hot-film sensor.

## 3. Experimental set-up

A local controller, consisting of one sensor and three actuators, as shown in figure 6, was built to test the control scheme described. The streamwise stations of the excitation source, the sensor and the actuators were 410 mm, 510 mm and 530 mm downstream from the leading edge of the flat plate respectively, using the same arrangement as in the numerical modelling.

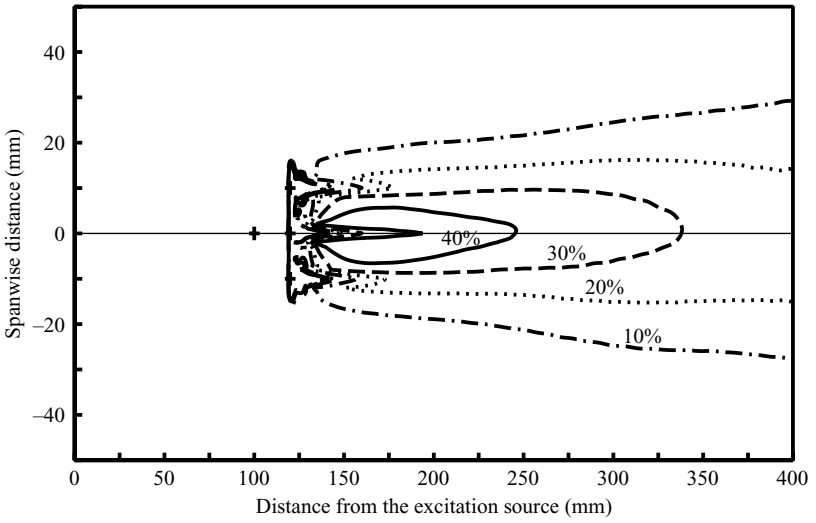


FIGURE 7. Same as figure 6, except that the control signal is not pure but at the signal-to-noise ratio (SNR) of 10:1.

### 3.1. *The experimental facilities*

All the experiments were carried out on a flat plate mounted vertically in the 3 ft square working section of the low-noise low-turbulence closed-return wind tunnel at the Engineering Department, Queen Mary, University of London. Details of the wind tunnel have been described by Gaster & Shaikh (1996). With the plate model mounted, the flow was uniform and the turbulence intensity of the free-stream turbulence was less than 0.01 % at the required speed in the frequency range of 2 Hz to 2 kHz. The flat plate was 1.65 m in length and 9 mm thick and was fitted with an elliptic leading edge of length 63 mm which had an asymmetric geometry with a ratio 1:2 of thickness on the working side to the non-working side. The overall distribution of pressure over the plate was set by the angle of the plate to the incident flow, but fine adjustment was provided by a flap and a small tab that were mounted at the trailing edge of the plate. With this system an almost zero pressure gradient was obtained and the stagnation point was positioned just on the working side of the plate. A removable 260 mm diameter circular disk was mounted on the centreline 500 mm downstream from the leading edge. An array of spanwise small loudspeakers (15 speakers with spanwise spacing of 10 mm), 410 mm downstream from the leading edge, was buried in the disk. Each speaker was controlled by one of the outputs of a 16-bit digital module fed with a series of computer-generated random binary numbers. Fifteen operational amplifiers were used to control the voltage levels of the speakers. The speakers communicated with the flow through holes of 0.5 mm diameter. The sensor and three actuators were also fitted in the disk.

Constant-temperature hot-wire anemometry was used to measure the flow in the boundary layer. The probe was of the boundary-layer type with a 2.5 μm gold-plated tungsten wire (Dantec 55P05). The position of the hot wire was driven by a three-dimensional traverse system using stepper-motors.

### 3.2. *Sensors and actuators*

After considering the sensitivities and SNRs of microphones (pressure sensor), hot films and hot wires, hot-wire probes with only the wire and the prong portions

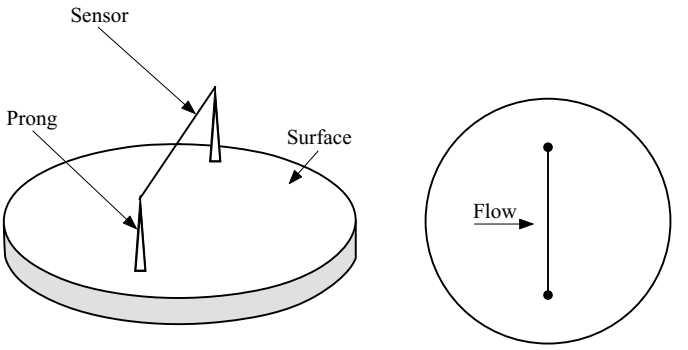


FIGURE 8. Schematic diagram of the hot-wire probe protruding into the boundary layer above the plate surface. This hot wire was used in the real-time implementation.

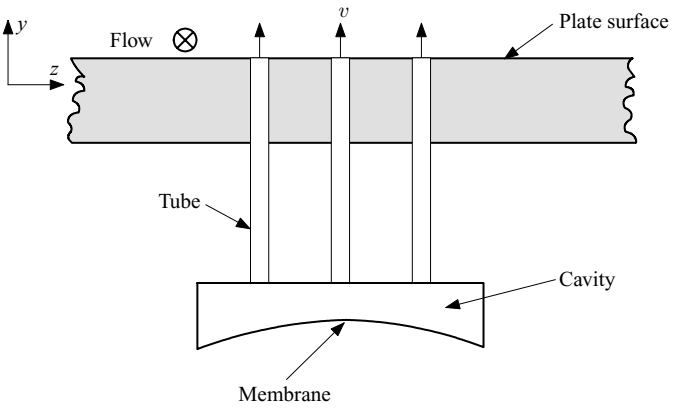


FIGURE 9. Schematic diagram of the oscillating jet-type source actuators. Three actuators were driven by one speaker and positioned side by side in the spanwise direction with a separation of 10 mm.

protruding into the flow were chosen as upstream sensors to detect the on-coming disturbances. This kind of device has been used by Rebbeck & Choi (2001). A schematic diagram of the hot-wire plug is shown in figure 8. The wire was positioned 0.4 mm above the plate surface. The wire and prongs will, of course, modify the mean velocity profile and could therefore alter the stability characteristics of the resulting boundary-layer flow. But it turned out that the effect was very small and could safely be ignored a few millimetres downstream of the hot wire. This type of hot-wire sensor can easily be made and has very high sensitivity and good SNR.

Actuation of the cancelling disturbances had to be achieved with devices integrated into the boundary wall. Gaster (2000) showed that stronger cancelling signals were more easily generated by an unsteady normal jet-like source than by an unsteady bump, and this type of actuator was therefore chosen. The same small speakers used to introduce the upstream disturbances were also selected for the control actuators and fitted into the disk with an exit hole of 1 mm diameter. The actuators are schematically illustrated in figure 9 and the corresponding frequency response of the actuators is shown in figure 10. The data were recorded 0.4 mm above the exit of the actuator driven by different frequency excitations with the same voltage level. When the frequencies were less than 50 Hz, or more than 400 Hz, the response was poor.

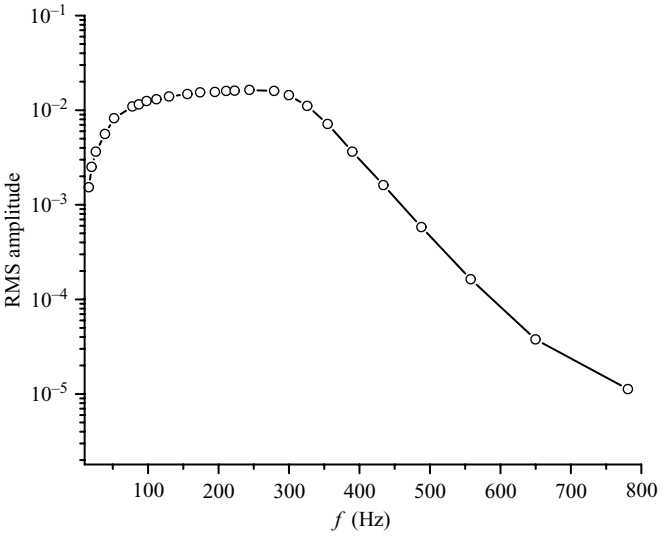


FIGURE 10. RMS amplitudes of the hot-wire records measured at the output of the actuator driven by different frequency excitation at the same voltage level.

But the figure shows that the actuators had a reasonably flat frequency response over the range required.

### 3.3. *Data processing*

The boundary layer was artificially excited by the same stored excitation record a number of times at each measurement location so that the ensemble-averaged response could be obtained to improve the SNR of the hot-wire data. The noise below 20 Hz was large and despite the ensemble averaging this component was not completely removed. In this investigation our interest was focused on relatively high frequencies of the T-S waves. The output of the hot-wire anemometer was preamplified and passed through a 20 Hz to 2 kHz band-pass filter before being sampled by the A/D converter at the rate of 2 kHz.

## 4. Experimental results

### 4.1. *Active off-line control*

The first stage of the experiment was carried out off-line. The aim of off-line control was to validate the numerical modelling so that a practical scheme for *real-time* implementation could be chosen. By recording the sensor signals a number of times for the same excitation pattern (128 times for the wavepacket and 32 times for the three-dimensional random disturbances in the experiment) a relatively noise-free sensor signal was formed. The driving signal to be fed to the actuators was then calculated off-line for any of the desired control strategies. The signal was then stored in the D/A converter and the experiment repeated with the same excitation using the stored control signal to drive the actuators.

Since the driving signal was stored in the off-line control process, it was not necessary to use a fixed hot-wire wall probe. Instead, the traversable single hot wire was used to detect the on-coming signal at the non-dimensional height $\eta = 0.5$ ($y = 0.4$ mm) above the plate at the position $x = 510$ mm. When the control was activated, the hot wire was moved downstream so that the disturbance field was clean.

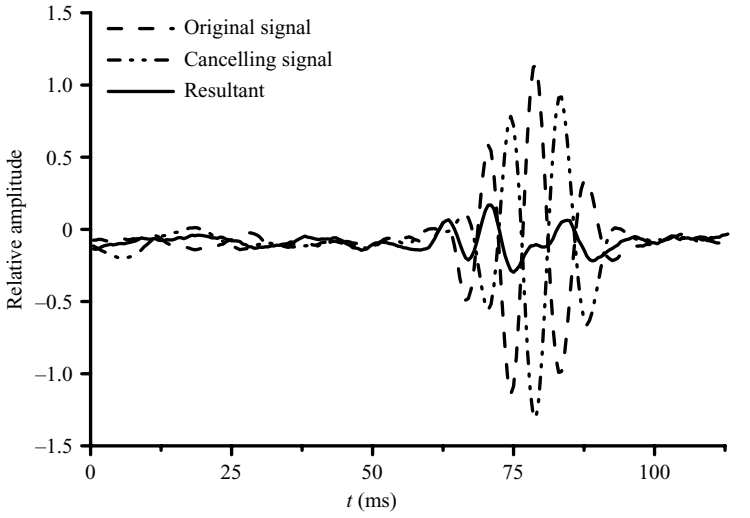


FIGURE 11. Boundary-layer responses to an impulse with and without control (off-line) using the uncoupled transfer function (mode 1). Data were measured by the hot wire at $x = 760\,\text{mm}$, $\eta = 0.5$ on the centreline.

4.1.1. *Cancellation of wavepackets*

The boundary layer was first excited by the small speaker on the centreline using a series of computer-generated impulses at intervals of 0.1 s so that the wavepackets behaved like isolated events. Typical results on the centreline at $x = 760\,\text{mm}$ with and without control using mode 1 are shown in figure 11. The signals were obtained in one of the three ways: by introducing the wavepacket with no control (original signal); by driving the actuator without an upstream on-coming disturbance (cancelling signal); and by both upstream disturbance forcing and downstream control (resultant). The figure shows that the magnitude of the resultant wavepacket was significantly reduced, leaving a weak residue. The percentage reduction in the amplitude of disturbance was found to be around 75 % and the corresponding correlation coefficient was about 0.98, which are almost the same as that given by the numerical model.

The other two simple transfer functions, shown in figure 5($b$, $c$), were also tested using the wavepacket excitation. Figure 12 shows the spanwise structures of the wavepackets under the control of the three modes at the same streamwise position. Both the calculations and the measurements are shown together. It should be noted that the ripple frequency is lower in the experiment, presumably because we are using a parallel-flow model scaled by the boundary-layer thickness at the source. The predicted residues after applying control modes 1,2 and 3 are shown on ($b$), ($c$) and ($d$). Most cancellation occurs, as expected, over the central region. The measurements obtained with the three types of control show very similar behaviour to that predicted even though the frequencies differ somewhat from the effects of boundary-layer growth.

4.1.2. *Cancellation of a fully three-dimensional random field*

Of great practical interest is the control of naturally excited disturbances. Here the type of on-coming disturbance arising with natural excitations was artificially produced by 15 small speakers distributed across the span. The magnitudes of the

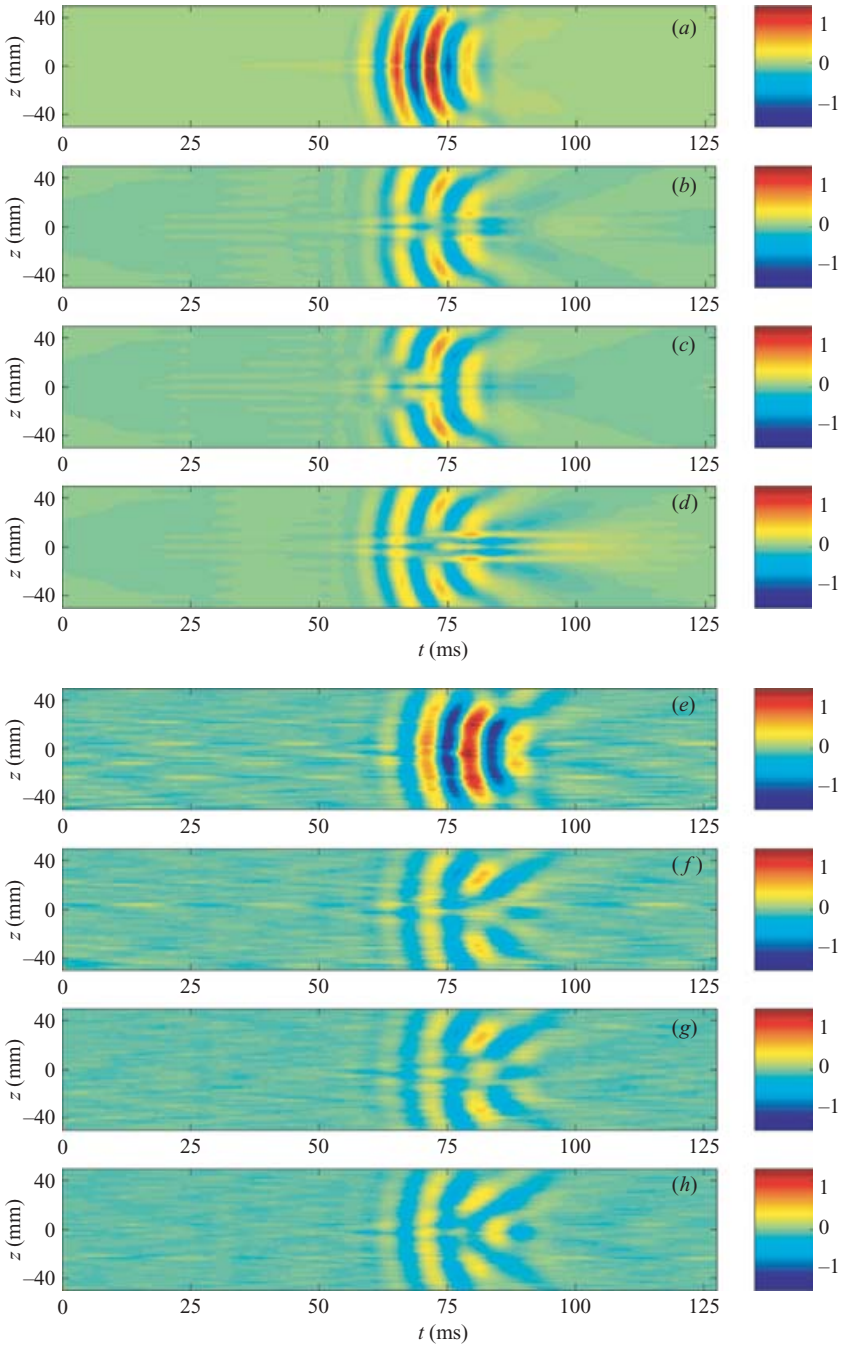


FIGURE 12. Space–time waveforms of wavepackets at $x = 760\,\text{mm}$, $\eta = 0.5$ from both the calculations (*a–d*)and the hot-wire measurement (*e–h*). (*a*, *e*) Original wavepacket and (*b–d*, *f–h*) results after cancellation using the three different control modes 1, 2, 3 respectively.

signals feeding each speaker were properly adjusted to produce a reasonably uniform three-dimensional field. It was found that the deviation of the amplitudes was less than 5 %, which is quite adequate for the purpose of the control experiment.

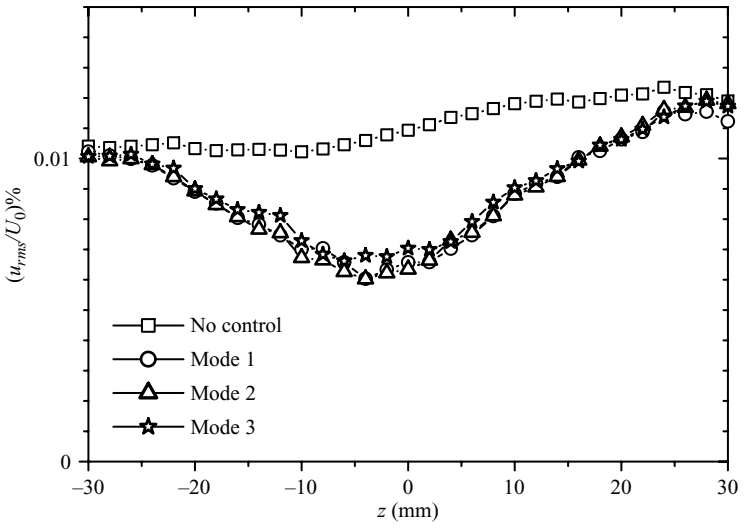


FIGURE 13. Spanwise distributions of the RMS amplitudes of the velocity fluctuations ($u_{rms}$) with and without the three control modes. Data were recorded at $x = 650$ mm, $\eta = 0.5$.

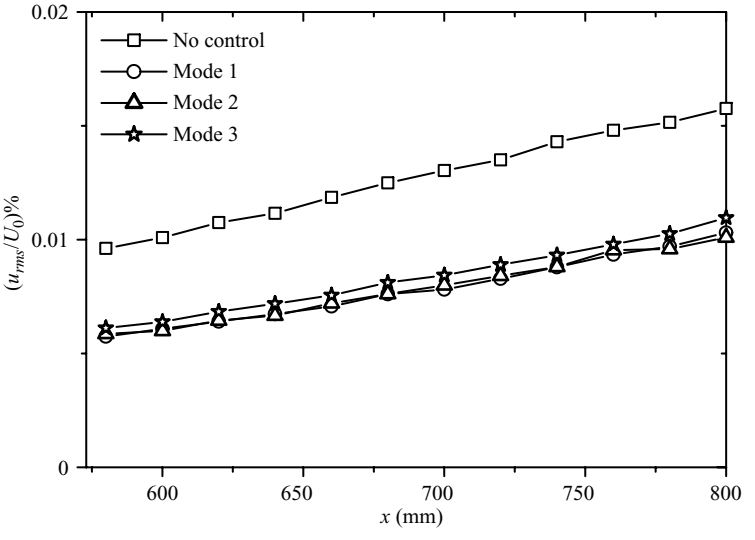


FIGURE 14. Streamwise variation of the RMS amplitudes of the velocity fluctuations ($u_{rms}$) with and without the three control modes. Data were recorded on the centreline at $\eta = 0.5$.

Figure 13 shows the spanwise distributions of the RMS amplitudes ($u_{rms}$) of the disturbances with the three different control modes together with the uncontrolled measurement. Considerable reduction in the disturbance amplitude over the central area was obtained in all cases and the differences between them was quite small. The reductions in $u_{rms}$ degraded gradually with spanwise distance. Figure 14 shows the streamwise variation of the $u_{rms}$ amplitudes on the centreline at a fixed height above the plate. The downstream evolution of the residues after cancellation grew linearly in the control region in a similar manner to the uncontrolled disturbance. Modes 1

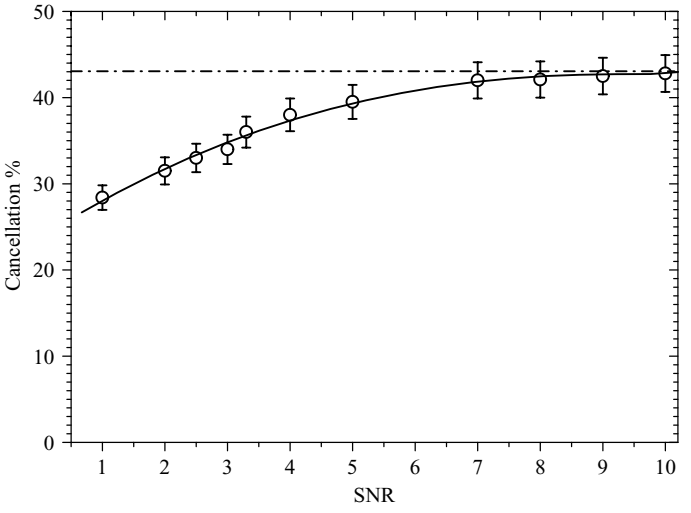


FIGURE 15. Percentage cancellation in $u_{rms}$ using the driving signal at the different SNRs. Data were recorded at $x = 650\,\text{mm}$, $\eta = 0.5$ on the centreline.

and 2 show almost the same degree of cancellation, while mode 3 indicates a slightly degraded performance.

The hot wire had large SNR and the sensor signal could therefore be considered to be relatively clean. The effect of external noise on the performance of the control system was tested. The driving signal was contaminated by external noise within the frequency range of unstable T-S waves. Figure 15 shows the percentage change in $u_{rms}$ at the position of $x = 650\,\text{mm}$ and $\eta = 0.5$ on the centreline. The cancellation was degraded to some extent at low values of SNR. However, when the SNR was greater than 7:1 the cancellation was unaffected.

### 4.2. *Active real-time control*

The sensor signal was obtained by the fixed hot-wire probe mounted on the surface. Although the sensor signal could no longer be averaged, the records detected by the traversable hot wire at the downstream target position were still ensemble-averaged to reduce variability. A digital control system was built to transform the sensor's signal into a control signal by convoluting the signal with the two-spike transfer function. The digital system processing (DSP) sampled at the rate of 2 kHz, which was around 10 times the highest frequency of interest. The programme was written in assembler language in order to make it sufficiently fast.

Figure 16 shows the percentage reduction in $u_{rms}$ of the fully three-dimensional random field comparing the calculation and the measurements under both the off-line and real-time processes. The raw estimates required smoothing to reduce variability and this was carried out by applying Hanning weights. The calculation was weighted in the same way to provide a proper comparison. The figure shows a very good quantitative agreement between the calculation and the experimental measurements. In the real-time implementation, the sensor signal was not ensemble-averaged and no doubt the SNR was much smaller than that in the off-line control. However, almost the same cancellation was obtained from the real-time implementation as in the off-line process, indicating that the external noise was not a serious problem.

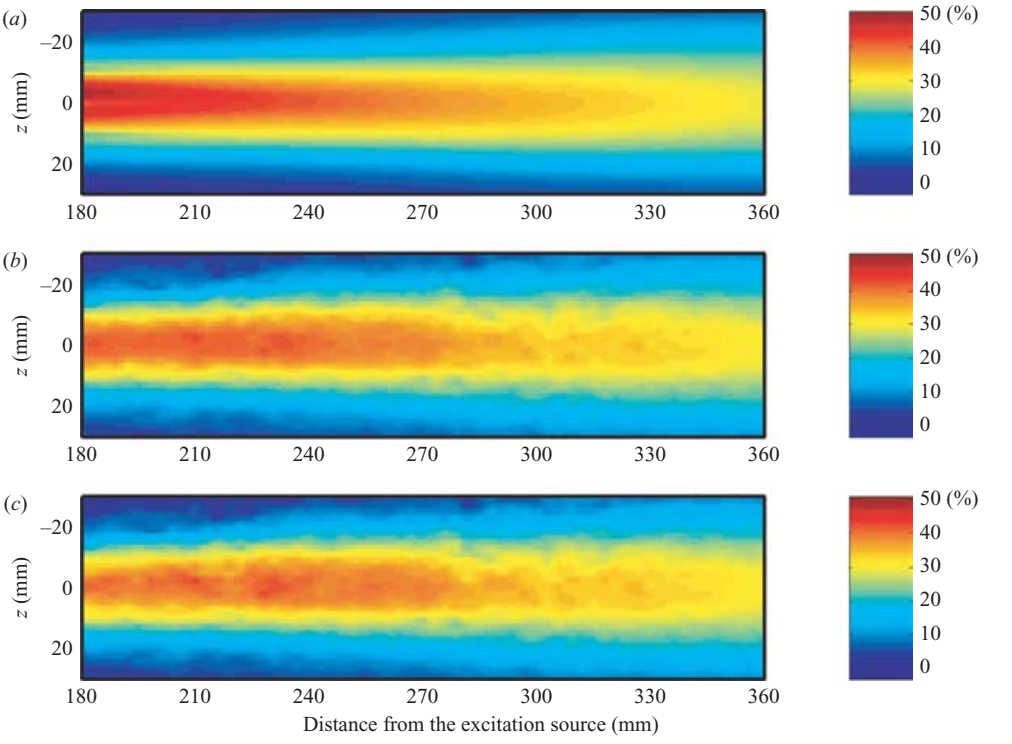


FIGURE 16. Percentage reduction in $u_{rms}$ of the fully three-dimensional random disturbances on the plane of $\eta = 0.5$ above the plate surface. (*a*) Calculation; (*b*) measurement (off-line); (*c*) measurement (real-time).

## 5. Discussion

The formulation and implementation of an active control of spatially evolving three-dimensional boundary-layer instability waves has been considered. Numerical modelling of the disturbances in the boundary layer, using linear theory and the parallel-flow approximation, was employed to determine possible transducer geometries, the transfer function linking the actuator driving signals with the upstream sensors and the effectiveness of various control schemes.

The modelling showed that the transfer function could be discretized so that a practical spanwise spacing of 10 mm could be used without any significant loss in control. Also it was found that the transfer function could be approximately represented by the values along the centreline, effectively ignoring any cross-linking over the span. Further simplification was achieved by approximating this function by a two-spike function, with their amplitudes suitably tuned. Indeed, reducing this transfer function to a single spike, or just a time delay, also provided a very good degree of control. Excellent cancellation from an on-coming three-dimensional perturbation field was predicted, even with the simplified approximate transfer functions.

It was not possible with the instrumentation available to experimentally validate these predictions for an array of detectors and actuators. It was therefore proposed to investigate experimentally the effect of a single control element with single sensor and three actuators. The numerical scheme was used to predict the effect of such an elemental control device on the three-dimensional disturbance field. A small zone behind the control element showed some reduction in disturbance level.

Experimental confirmation of these predictions was carried out in two stages. First, off-line processing was used that enabled the controlling signal to be evaluated off-line, avoiding any difficulties arising from real-time processing. This approach relied on the fact that the disturbance field to be cancelled was created far upstream by a spanwise array of exciters buried in the flat plate. Computer-generated signals were used to create deterministic and repeatable excitations of various forms. One experiment enabled the sensor signal to be measured and then a repeat experiment, using the same excitation, was carried out with the desired control signal. Experiments using isolated impulse excitations from one point source and a fully three-dimensional random-disturbance field were performed. The results showed that all control strategies tested provided the degree of control close to the predictions. The simplified transfer functions that were modelled by either two or a single delta function were also almost equally successful.

Secondly, a real-time digital controller was built and used to confirm the off-line experiments and the modelling predictions.

The original fully three-dimensional upstream random excitation was generated by a superposition of wavepackets from different spanwise locations at random time instants. It is not, therefore, unreasonable to expect that the amplified version of the disturbance field that developed downstream could also be synthesized by a suitable superposition of wavepackets. Far downstream the asymptotic form of a wavepacket is defined by the phase and amplitude of the ripple at the centre. Therefore sufficiently far downstream, where the wavepacket can be expected to be governed by the asymptotic form, a transfer function consisting of two spikes seems appropriate. The two spikes are required to control both the phase and peak position. Since the phase and group velocities differ by only a small amount the additional approximation to a single-spike transfer function may be a reasonable approximation.

## 6. Concluding remarks

We have shown that the simple linear numerical scheme can provide useful guidance as to the observed behaviour of a practical control system in a wind tunnel. The numerical approach provided an essential tool for determining the geometries of transducers and for estimating the required transfer functions.

Although only an isolated controller was tested the results were so well modelled that extrapolation to a situation with a large number of elemental devices seems feasible. It can then be expected that excellent suppression of instability waves could be achieved over a significant area of the flow. The scheme was shown, both numerically and experimentally, to be insensitive to system noise.

The work was supported by British Aerospace and resulted in a PhD thesis (Li 2004). The authors would also like to acknowledge the technicians of Aeronautical lab for their help in constructing the instruments used in this project.

## REFERENCES

Biringen, S. 1984 Active control of transition by periodic suction-blowing. *Phys. Fluids* **27**, 1345–1347.

Bewley, T. R. 2001 Flow control: new challenges for a new renaissance. *Prog.Aero.Sci.* **37**, 21–58.

Bewley, T. R. & Liu, S. 1998 Optimal and robust control and estimation of linear paths to transition. *J. Fluid Mech.* **365**, 305–349.

Bower, W. W., Kegelman, J. T., Pal, A. & Meyer, G. H. 1987 A numerical study of two-dimensional instability-wave control based on the Orr-Sommerfeld equation. *Phys. Fluids* **30**, 998–1004.

Braslow, A. L. 1999 *A History of Suction-type Laminar Flow Control with Emphasis on Flight Research*. Monographs in Aerospace History, NASA History Division Office of Policy and Plans, NASA Headquarters, Washington, DC.

Gaster, M. 2000 Active control of boundary layer instabilities using MEMs. *Current Sci.* **79**, 774–780.

Gaster, M. & Shaikh, F. N. 1996 Receptivity of free-stream disturbances. *Final Report*, MOD Grant ref.2029/280 RG 16019.

Gmelin, C. & Rist, U. 2001 Active control of laminar-turbulent transition using instantaneous vorticity signals at the wall. *Phys. Fluids* **13**, 513–519.

Högberg, M. & Henningson, D. 2002 Linear optimal control applied to instabilities in spatially developing boundary layers. *J. Fluid Mech.* **470**, 151–179.

Joslin, R. D., Erlebacher, G. & Hussaini, M. Y. 1996 Active control of instabilities in laminar boundary layers-overview and concept validation. *Trans. ASME: J. Fluids Engng* **118**, 494–497.

Joslin, R. D., Nicolaides, R. A., Erlebacher, G., Hussaini, M. Y. & Gunzburger, M. D. 1995 Active control of boundary-layer instabilities: use of sensors and spectral controller. *AIAA J.* **33**, 1521–1523.

Kleiser, L. & Laurien, E. 1985 Numerical investigation of interactive transition control. *AIAA Paper* 85-0566.

Kral, L. D. & Fasel, H. F. 1991 Numerical investigation of three-dimensional active control of boundary-layer transition. *AIAA J.* **29**, 1407–1417.

Laurien, E. & Kleiser, L. 1989 Numerical simulation of boundary layer transition and transition control. *J. Fluid Mech.* **199**, 403–440.

Li, Y. 2004 Active control of boundary-layer instabilities. PhD Thesis. Queen Mary, University of London.

Liepmann, H. W., Brown, G. L. & Nosenchuck, D. M. 1982*a* Control of laminar-instability waves using a new technique. *J. Fluid Mech.* **118**, 187–200.

Liepmann, H. W., Brown, G. L. & Nosenchuck, D. M. 1982*b* Active control of laminar-turbulent transition. *J. Fluid Mech.* **118**, 201–204.

Milling, R. 1981 Tollmien-Schlichting wave cancellation. *Phys. Fluids* **24**, 979–981.

Opfer, H., Evert, F., Ronneberger, D. & Grosche, F. R. 2003 On the potential and the limitations of boundary-layer stabilisation via active wave cancellation. In *Recent Results in Laminar-Turbulent Transition* (ed. S. Wagner, M. Kloker & U. Rist). Notes on Numerical Fluid Mechanics and Multidisciplinary Design, Vol. 86, pp. 219–230. Springer.

Pal, A., Bower, W. W. & Meryer, G. H. 1991 Numerical simulations of multi-frequency instability-wave growth and suppression in the Blasius boundary layer. *Phys. Fluids* A **3**, 328–340.

Saric, W. S. 1992 Laminar-turbulent transition: fundamentals. *AGARD* R-786, *Special Course on Skin Friction Drag Reduction.*

Rebbeck, H. & Choi, K. S. 2001 Opposition control of near-wall turbulence with a piston-type actuator. *Phys. Fluids* **13**, 2142–2145.

Sturzebecher, D. & Nitsche, E. 2003 Active control of boundary-layer instabilities on an unswept wing. In *Recent Results in Laminar-Turbulent Transition* (ed. S. Wagner, M. Kloker & U. Rist). Notes on Numerical Fluid Mechanics and Multidisciplinary Design, Vol. 86, pp. 189–202. Springer.

Thomas, A. S. W. 1983 The control of boundary-layer transition using a wave-superposition principle. *J. Fluid Mech.* **137**, 233–250.

Walther, S., Airiau, C. & Bottaro, A. 2001 Optimal control of Tollmien-Schlichting waves in a developing boundary layer. *Phys. Fluids.* **13**, 2087–2096.